# A study on elasto-plastic raft foundation-soil interaction

## L'étude de l'interaction élasto-plastique entre le radier de fondation et le sous-sol

M.Gryczmański & S.Majewski – *Technical University of Silesia, Gliwice, Poland*

ABSTRACT: The elasto-plastic material model with two-parameter isotropic hardening/softening rule is presented. Due to unified description of material behaviour both in elastic and post-elastic stadium the model can be adopted to the analysis of soil, as well as concrete and reinforced concrete elements and structures. Therefore it is very efficient in the analysis of soil-structure interaction problems. A sample of such an analysis - calculations of the square raft foundation co-operating with subsoil block - is presented in the paper.

RÉSUMÉ: Dans ce travail on présente l'élasto-plastique modele constitutif avec deux parametres isotrope de la fortification de l'affaiblissement. Grâce a la description uniforme du materiel qui se conduit également dans le stade élastique et post-élastique, le modele peut etre adapté aux analyses de sous-sol et aussi aux éléments des constructions du béton et du béton armé. Et c'est pourquoi ce modele est trés effectife dans l'analyse des problemes d'interaction statique du systeme: „construction-sol„. On y présente aussi l'essai de l'analyse de calcules de la collaboration : le panneau carré de fondation avec du sous-sol.

## 1. INTRODUCTION

Idealisation of very complex mechanical soil behaviour must be kept in some reasonable limits. In the light of recent investigations (see e.g. Atkinson and Salffors, 1991) such properties as sensitivity of stiffness characteristics on stress history and low strain level should not be neglected nowadays even in design analysis of foundation-subsoil interaction under monotonic working loads. For this purpose material constitutive modelling within isotropic hardening plasticity approach, best in the framework of the critical state soil mechanics presented by Schofield and Wroth including "cap" concept proposed by Di-Maggio and Sandler seems to be necessary. At present, similar constitutive assumption is more and more often applied to concrete (see e.g. Chen). This leads to an unified description of materials behaviour in soil-structure interaction analysis. The differences between various materials are reduced just to the level of parameters.

The above approach applied to interaction problems implies incrementally-iterative finite elements solution. Regarding mostly three-dimensional geometry, these interaction tasks still are extremely difficult from analytical, as well as experimental point of view. Therefore, maybe, the analyses of this type are rather rarely published, in spite of their practical importance. Comprehensive, parametric studies of such cases are particularly necessary.

The attempt of elasto-plastic analysis of the raft foundation-subsoil system is undertaken in the report. For soil and concrete constitutive characteristics and extended "cap" model proposed by one of the authors (Majewski, 1994) is assumed. It is briefly described in section 2. The study comprises square raft foundation 10.0 m long and wide and 1.0 m thick subjected to the vertical forces transmitted by four symmetrically situated columns. More detailed description of the finite elements mesh and material parameters are given in section 3. Some results of the analysis and conclusions are discussed in section 4.

## 2. MATERIAL MODEL FOR SOIL AND CONCRETE

The unified constitutive model for materials involved in soil-foundation interaction was recently developed by one of the authors (Majewski, 1994). New, improved version of this model is presented in 1997.

In general it is an extended "cap" model with smooth combined yield surface and isotropic plastic hardening/softening dependent on two plastic strain invariants. Model is based on the following assumptions:

- the yield surface is composed of the part of paraboloid ( $F_1 = 0$ ), closed or opened from the compression side and the spherical cap in the tensile zone ( $F_2 = 0$ ),
- each of these formations, as the matter of fact, is not a single surface of revolution, but creates a set of such surfaces (paraboloids and spheres respectively, always with smooth transition from one to another); their radius is dependent on the third stress invariant (Lode's angle),
- both parts of surface evolve (expand or shrink) according to the changes of plastic components of the volumetric and deviatoric strains, $\varepsilon_v^{pl}$ and $\varepsilon_s^{pl}$ respectively,
- plastic flow rule is considered to be associated with the yield condition,
- as long as the stress remains inside the space limited by the yield surface, the material behave as non-linear elastic isotropic media, described by elastic, tangent shear and bulk moduli $G_t$ and $K_t$ respectively,
- the principal of additivity of elastic and plastic strain is valid.

Following equations express the above assumptions:

$$F_1 = q - \sqrt{3}\left(\beta Y^2 - 3\alpha Y p - \gamma\left(\frac{p}{p_c}\right)^2\right)\rho = 0 \tag{1}$$

$$F_2 = q^2 + 3\left(p - c_s\right)^2 - 3\frac{\beta^2 Y^4 \rho^2}{1 + 9\alpha^2 Y^2 \rho^2} = 0, \tag{2}$$

$$G_t = G_o p_a \left(\frac{p}{p_a}\right)^n \left(1 - \psi R_f\right)^2 \quad \text{for soil}$$
$$G_t = \frac{E_t}{2\left(1 + \nu_t\right)} \quad \text{for concrete} \tag{3}$$

$$K_t = K_o p_a \left(\frac{p}{p_a}\right)^m \quad \text{for soil}$$
$$K_t = \frac{E_t}{3\left(1 - 2\nu_t\right)} \quad \text{for concrete} \tag{4}$$

In equations (1) - (4) $p$ and $q$ are the mean and shear stresses defined as:

$$p=\frac{1}{3}(\sigma_x+\sigma_y+\sigma_z)$$

$$q=\frac{1}{\sqrt{2}}\left[(\sigma_x-\sigma_y)^2+(\sigma_y-\sigma_z)^2+(\sigma_z-\sigma_x)^2+6(\tau_{xy}^2+\tau_{yz}^2+\tau_{zx}^2)\right]^{\frac{1}{2}} \quad (5)$$

Some other notations are given in the Table 1 separately for soil and concrete.

Table 1.

| | Expression for soil | Expression for concrete | |
|---|---|---|---|
| $\alpha$ | $\frac{2\sin\Phi}{\sqrt{3}(3-\sin\Phi)}$ | $\frac{f_c-\frac{1}{m_o}f_t}{f_c+f_t}\cdot\frac{\sqrt{3}}{3}$ | (6) |
| $\beta$ | $\frac{6\cos\Phi}{\sqrt{3}(3-\sin\Phi)}c$ | $\frac{\left(1+\frac{1}{m_o}\right)f_c f_t}{\sqrt{3}(f_c+f_t)}$ | (7) |
| $\gamma$ | $\beta-3\alpha\gamma p_c$ | $\frac{\beta+21\alpha f_c}{500f_c^2}$ | (8) |
| $p_c$ | $p_{co}\exp\left(-\frac{\varepsilon_v^{pl}}{\lambda-\kappa}\right)$ if $\varepsilon_v^{pl}\le 0$<br>else<br>$\frac{p_{co}}{2}\left[1+\exp\left(-\frac{\varepsilon_v^{pl}}{\lambda-\kappa}\right)\right]$ | $p_{co}$ if $\varepsilon_v^{pl}\le 0$<br>else<br>$0.001+p_{co}\exp(-C_1\varepsilon_v^{pl})$ | (9) |

Another ones are presented below:

$$c_s=\frac{3\alpha\beta\gamma^3}{1+9\alpha^2\gamma^2} \quad (10)$$

$$Y=C_4+(1-C_4)(C_2\varepsilon_s^{pl}+1)\exp(-C_2\varepsilon_s^{pl}) \quad (11)$$

$$\rho=\frac{0.5+(m-0.5)\cos\frac{3\Theta}{2}}{\cos\Theta} \quad (12)$$

Furthermore, the tangential modulus of elasticity for concrete $E_t$ and Poisson's ratio $\nu_t$ for concrete are dependent on the shear stress level $\psi$ according to formulae:

$$E_t=\omega\sqrt{4\eta^2(1-\psi)+2\eta(2-3\psi+\psi^2)+1-2\psi+\psi^2} \quad p\le 0$$

$$E_t=2E_t\frac{\sqrt{3\psi^2-12\psi+9}}{3(2-\psi)} \quad p>0 \quad (13)$$

$$\nu_t=\nu_i \quad \text{for } \psi\le 0.8$$

$$\nu_t=(12.5-25\nu_i)\psi^2+(40\nu_i-20)\psi+8-15\psi \quad \text{for } \psi>0.8 \quad (14)$$

$$\psi=\frac{q}{q_f} \quad (15)$$

In these equations:

$$\omega=\frac{f_c}{\varepsilon_c(\eta+1-\psi)},\quad \eta=\frac{E_i\varepsilon_c-f_c}{2f_c-E_i\varepsilon_c} \quad (16)$$

Lode's angle $\Theta$ in equation (12) is defined as:

$$\Theta=\frac{1}{3}\arccos\left(\frac{3\sqrt{3}J_3}{2J_2^{\frac{3}{2}}}\right) \quad (17)$$

where $J_2$ and $J_3$ denote the second and third deviatoric stress invariants.

Coefficient $m$ in the same equation is equal:

$$m=\frac{r_t}{r_c}=1-(1-m_o)\exp\left(\frac{\sigma_m}{10f_c}\right) \quad (18)$$

while:

$$m_o=\frac{r_t^o}{r_c^o}=\frac{3-\sin\Phi}{3+\sin\Phi},\qquad \Phi=\arcsin\left[\frac{3(f_c-f_t)}{3f_c+f_t}\right] \quad (19)$$

Plastic components of volumetric and distortional strains $\varepsilon_v^{pl}$ and $\varepsilon_s^{pl}$ in equations (9) and (11) are given by formulae:

$$\varepsilon_v^{pl}=\varepsilon_x^{pl}+\varepsilon_y^{pl}+\varepsilon_z^{pl}$$

$$\varepsilon_s^{pl}=\frac{\sqrt{2}}{2}\left\{\left(\varepsilon_x^{pl}-\varepsilon_y^{pl}\right)^2+\left(\varepsilon_y^{pl}-\varepsilon_z^{pl}\right)^2+\left(\varepsilon_z^{pl}-\varepsilon_x^{pl}\right)^2+\right.$$
$$\left.+\frac{3}{2}\left[\left(\gamma_{xy}^{pl}\right)^2+\left(\gamma_{yz}^{pl}\right)^2+\left(\gamma_{zx}^{pl}\right)^2\right]\right\} \quad (20)$$

For soil model is quantified by 10 material parameters: pre-consolidation pressure $p_{co}$, internal friction angle $\Phi$, cohesion factor $c$, Duncan's model constants $G_o, K_o, R_f, m, n$ and Modified Cam-clay ones $\lambda$, and $\kappa$. Coefficients $C_2, C_3, C_4$ are assumed here to be equal zero.

The behaviour of concrete if determined by another 9 parameters: the uniaxial compressive and tensile strengths $f_c$, $f_t$, the ratio of tensile to compressive meridians in the $\Pi$-plane $m_o$, initial values of the modulus of elasticity and Poisson's ratio $E_i$ and $\nu_i$, the extreme compressive strain in the uniaxial compression $\varepsilon_c$, and hardening/softening constants $C_2, C_3, C_4$.

Considering the simulative ability of the model it's worthy to notice, that the paraboloidal yield surface $F_1=0$ for $\gamma>0$ is closing admissible stress field from the compression side like in the Modified Cam-clay and other models from critical state family (Gryczmański, 1995). Thus the plastic behaviour of cohesive soils for the pre-critical states can be realistically described. On the other hand, the open conical surface for $\gamma=0$ seems to be applicable for sands. Assumption $C_2=C_4=0$ for soils means neglecting distorsional hardening/softening and return to the classical critical state soil mechanics dependent on the volumetric hardening only. Assuming $C_2\neq 0$, $C_4\neq 0$ softening of concrete in post-critical state state can be taken into account.

## 3. SAMPLE CALCULATIONS OF THE RAFT FOUNDATION-SOIL INTERACTION

The material model described in the previous section is applied in the software package MAFEM, which was created mainly for the analysis of soil-structure interaction problems, but was also successfully used in the calculations of different concrete, reinforced concrete and masonry structures. This package was used to the analysis of square reinforced concrete slab 10.0·10.0m wide and 1.0m thick. Finite elements mesh over a quarter of this slab and co-operating subsoil block is presented in fig. 1.

All the 3-D interactive soil-structure system was devided into 432 solid 8-nodes elements. Total number of nodes was equal 647. The slab reinforcement of intensity 20.00cm$^2$/m was represented by linear bar elements running along the network axis on the upper and lower surface. Elasto perfectly plastic material model was assumed for steel.

The slab is loaded by four columns. The total force from each column Q=2750kN is distributed onto four nodes (fig. 2). In the first step of the incremental iterative procedure the dead load of soil and foundation was applied. The force realised by columns was given in following 9 steps so, that the force increment initially was equal 500kN in steps 2 and 3 and was lowered to 250kN in last 7 steps.

Three models were analysed:

- MEL - elastic model both for soil and concrete,
- M10 - elasto-plastic model of soil and concrete with strongly pre-consolidated soil ($p_{co}$=1.0MPa),
- M03 - elasto-plastic model of soil and concrete with lower pre-consolidation pressure ($p_{co}$=0.3MPa).

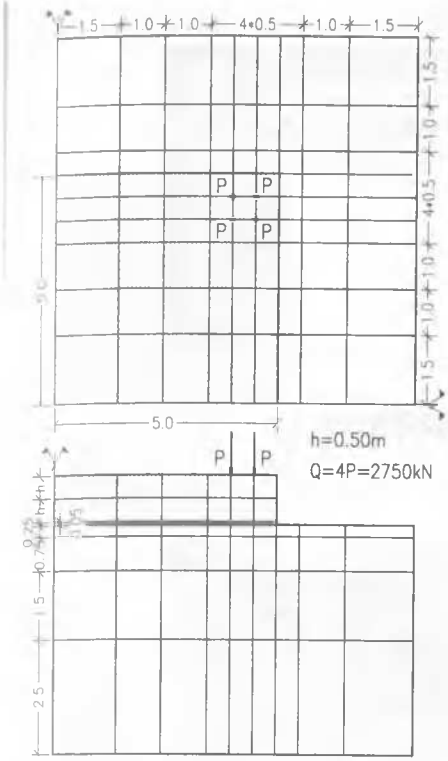


Fig.1. Finite elements mesh and dimensions

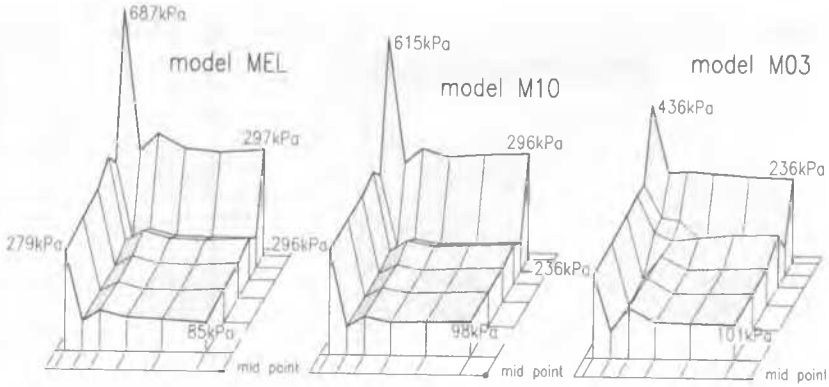


Fig. 2. Distribution of normal stress under the foundation. Models MEL, M10, M03

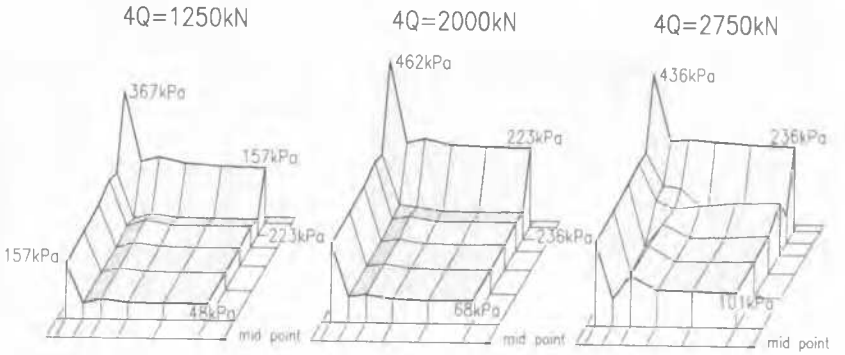


Fig. 3. Distribution of normal stress under the foundation. Model M03 - different load

Following parameters were assumed:

- for soil in model M10:

$K_o = 300, G_o = 135, m = n = 0.5, R_f = 0.8, \Phi = 35^o, c = 0.02\,MPa$

$p_{co} = 1.00\,MPa, \lambda = 0.015, \kappa = 0.005, C_2 = C_4 = 0.00$

- for soil in model M03:

$K_o = 300, G_o = 135, m = n = 0.5, R_f = 0.8, \Phi = 35^o, c = 0.02\,MPa$

$p_{co} = 0.30\,MPa, \lambda = 0.0045, \kappa = 0.0015, C_2 = C_4 = 0.00$

- for reinforcement:

$E = 205000\,MPa, \quad f_y = 250\,MPa, \quad f_r = 400\,MPa$

- for concrete:

$K = 12472\,MPa, \; G = 9354\,MPa$, (for $E_i = 22450\,MPa, \nu_i = 0.2$),

$f_c = 25\,MPa, f_t = 1.92\,MPa, \varepsilon_c = 0.0022,$

$C_1 = 1000, C_2 = 8.0 f_c^2, C_4 = 0.05$

In the elastic model MEL same parameters for concrete and soil, however without any limitation according to failure were assumed.

In the contact plane between the soil and foundation thin layer interface elements with same parameters as the corresponding soil were introduced.

Some results of the calculations are presented in figures 2-4.

The distribution of normal stress under one quarter of the foundation for all analysed model at the extreme load Q=2750kN in the axonometric view is presented in the fig. 2. As it was expected high stress concentration is observed on the edges of the foundation and particularly near its corners, while nearly uniform stress distribution is revealed in the middle part. Edge and corner stress decreases and the middle stress increases in slightly consolidated soil due to large area of plasticization. The same phenomenon is responsible for the effect, which can be observed in fig. 3. The extreme value of corner stress occurs at Q=2000kN, then the load increase results only in the increase of stress in the middle part of the foundation. It's worthy to observe some disturbance in the uniform distribution of normal stress under the foundation in the vicinity of edges in the model M03 with slightly pre-consolidated soil.

This disturbance isn't observed in the M10 model with heavily pre-consolidated soil. In fig.4 the distribution of normal and shear stress, as well as the effort level $\psi$ (see formula 15) under the foundation in models M10 and M03 in the last load step (Q=2750kN) is presented in the form of "maps" over one quarter of the analysed foundation. Very regular pattern of normal stress isolines in model M10 in contrary to model M03 was revealed. Two central maps in the same figure show the distribution of shear stress. The extreme shear stress in M10 model was 78kPa and only 48kPa in model M03. The distribution of shear stress in both model significantly differs. In model with heavily pre-consolidated soil (M10) the extreme shear stress appears just near the corners of the slab, while in model M03 it occurs in quite another place.

Two lower maps in the fig. 4 present the effort level $\psi$ just beneath the foundation (2.5cm) for models M10 and M03 in the last load step. All black area on the map of M03 model indicates elements, which reached the critical state. Full bearing capacity in the model with heavily pre-consolidated soil was observed only in one corner element under the foundation and also in few soil elements in the vicinity of slab corners (these are not shown in the figure). Obviously much more elements have reached this state in model M03.

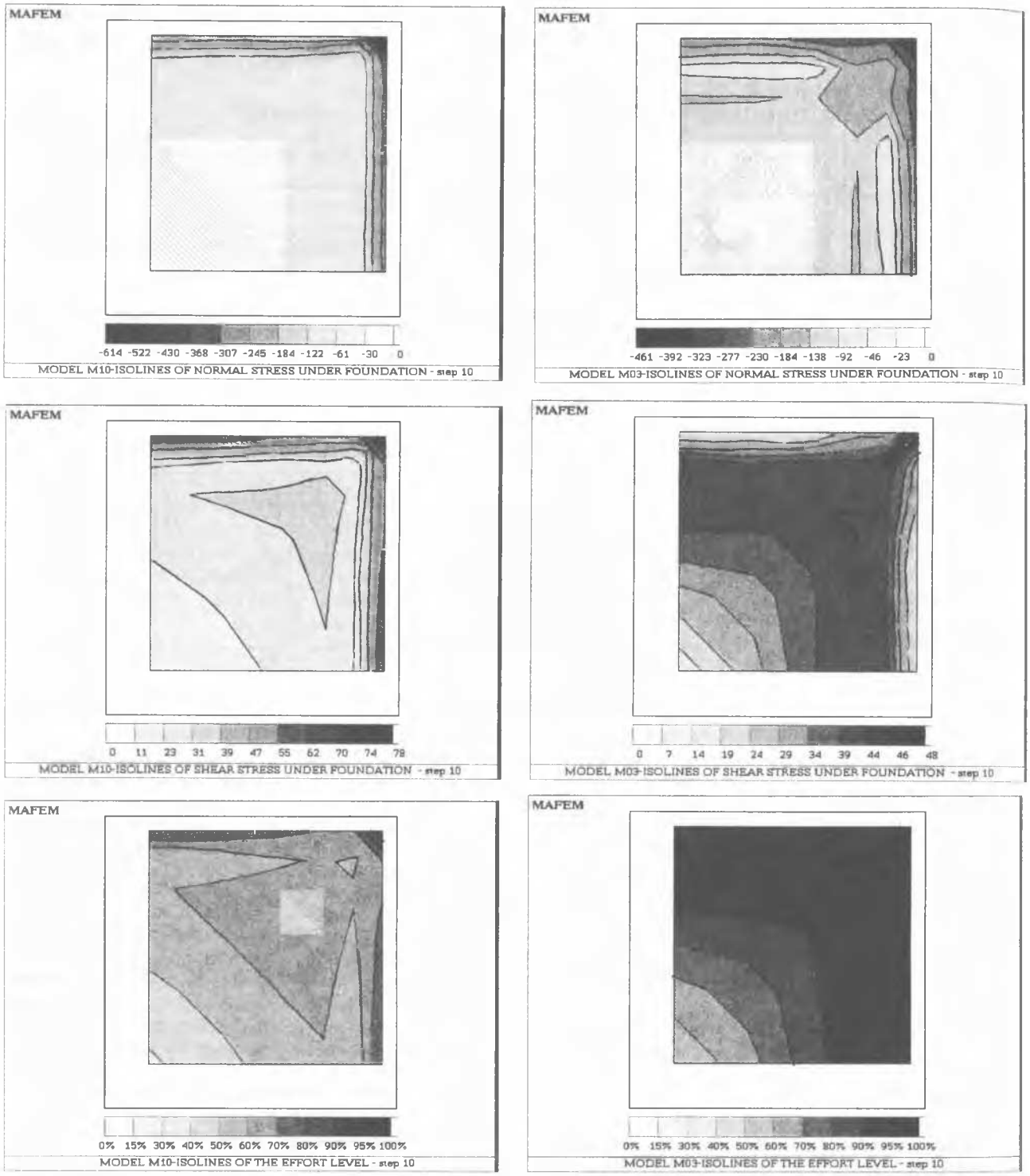


Fig. 4. Maps of distribution of the normal (upper) and shear stress under the foundation (central) and maps of the effort level (lower) over one quarter of the foundation. Models M10 and M03, full load.

## 4. CONCLUSION

The simple case of soil-foundation interaction was analysed, so no revelations could be revealed. Yet the analysis proved the success of the presented material model, all the more because the calculations were run at PC Pentium 150 computer. This confirms the efficiency of the presented model and of software package MAFEM, in which this model is applied. It is promising, that the elasto-plastic analysis can be introduced into the design practice, though there is still a lot of analytical and experimental work to be done before it.

## REFERENCES


Atkinson J.H., Sallfors G.: Experimental determination of stress-strain-time characteristics in laboratory and in situ tests. *General report, Proc. 10th ECSMFE*, Firence1991, Vol.3, 915-956

Majewski S.: Elasto-Plastic Double-Cap-Model for Structure-Subsoil Interaction Problems. *Archive of Civil Engineering*, Warsaw, vol. XL, z.3/4, 1994, pp.487-506.

Gryczmański M.: An introduction to elasto-plastic models for soils (in Polish). *Polska Akademia Nauk, Komitet Inżynierii Lądowej i Wodnej, IPTT*, Warszawa 1995 157 p.